



## Get Clarity On Generics

Cost-Effective CT & MRI Contrast Agents



FRESENIUS  
KABI

WATCH VIDEO

# AJNR

## MR Imaging and MR Spectroscopy in Rhizomelic Chondrodysplasia Punctata

Angèle Viola, Sylviane Confort-Gouny, Jean-Philippe  
Ranjeva, Brigitte Chabrol, Charles Raybaud, Francisca  
Vintila and Patrick J. Cozzone

This information is current as  
of August 19, 2025.

*AJNR Am J Neuroradiol* 2002, 23 (3) 480-483

<http://www.ajnr.org/content/23/3/480>

# MR Imaging and MR Spectroscopy in Rhizomelic Chondrodysplasia Punctata

Angèle Viola, Sylviane Confort-Gouny, Jean-Philippe Ranjeva, Brigitte Chabrol, Charles Raybaud, Francisca Vintila, and Patrick J. Cozzone

**Summary:** A case of rhizomelic chondrodysplasia punctata was investigated with MR imaging of the brain and hydrogen-1 MR spectroscopy of the brain and blood. Areas with abnormal signal hyperintensity on T2-weighted images or hypointensity on T1-weighted images were detected in the subcortical white matter. MR spectroscopy of the brain showed that normal-appearing white matter was characterized by increased levels of mobile lipids and *myo*-inositol, reduced levels of choline, and the presence of acetate. The importance of these metabolic anomalies is correlated to the deficiency in plasmalogen biosynthesis.

Rhizomelic chondrodysplasia punctata (RCDP) is a peroxisomal disorder characterized by a deficiency in the biosynthesis of plasmalogens (1, 2). Several variants of the disease corresponding to distinct biochemical abnormalities, such as deficiencies in the activity of phytanoyl-coenzyme A (CoA) hydroxylase (EC 1.14.11.18), dihydroxyacetone phosphate (DHAP) acyltransferase (DHAPAT) (EC 2.3.1.42), alkyl-DHAP synthetase (EC 2.5.1.26), and 3-ketoacyl-CoA thiolase (EC 2.3.1.16) have been described (1, 2). Individuals with RCDP have skeletal abnormalities, including proximal limb shortening and characteristic facial dysmorphism. Cataract and impaired hearing are frequent. Mental retardation develops in patients with RCDP, and they do not thrive. At autopsy, the brain of persons with RCDP has a reduced number of neurons in the cortex. Although peroxisomal disorders, including Zellweger syndrome and neonatal adrenoleukodystrophy, have been characterized with MR imaging and MR spectroscopy (3), no MR spectroscopy investigations of the specific brain metabolic

changes associated with RCDP have been performed, to our knowledge. Previous MR imaging studies (4–7) have shown abnormalities in the white matter; these include increased signal intensity in the periventricular white matter (4, 5) and semiovale centrum (5) on T2-weighted images. Other investigators (6, 7) reported delayed myelination, especially in the occipital region.

We describe the case of a patient with DHAPAT deficiency. The disease was investigated with MR imaging and combined in vitro hydrogen-1 MR spectroscopy of the blood and in vivo <sup>1</sup>H MR spectroscopy of brain. The purpose of this study was to identify brain metabolism anomalies in RCDP.

## Case Report

This male neonate was the first child of healthy, unrelated parents. He was born at 38 weeks' gestation after an uneventful pregnancy by means of forceps-assisted delivery. His weight at birth was 2850 g; length, 47 cm; and head circumference, 33 cm. He had joint contractures, chondrodysplasia, and bilateral cataracts. His limb length was abnormal, and his feet had equinovarus deformity. Typical facial dysmorphism consisting of a broad nasal bridge was noted. Radiographs of the skeleton revealed punctate calcific stippling of joints localized in the shoulders, elbows, ribs, and ankles. Moreover, this patient showed signs of pain to any stimulation and had feeding difficulties that necessitated gastric drip-feeding. At echography, images of his brain showed mild ventricular dilatation. Clinical symptoms and skeletal abnormalities were highly suggestive of RCDP. This diagnosis was confirmed after an assessment of peroxisomal function. Reduced de novo plasmalogen biosynthesis in erythrocytes, a result of a deficiency in DHAPAT, was detected. Other peroxisomal functions, including levels of pipelicolic acid and phytanic acid, very-long-chain fatty acid profile, and the activities of alkyl-DHAP synthase and 3-ketoacyl-CoA thiolase, were normal.

When the patient was aged 16 days, a complete MR investigation was performed. This study was approved by the local ethics committee (La Timone Hospital, Marseille, France), and the neonate's parents provided written informed consent. MR imaging and MR spectroscopy of the brain were performed at 1.5 T with a Vision Plus system (Siemens, Erlangen, Germany). The patient was not sedated. The MR imaging protocol included T1-weighted imaging (700/15 [TR/TE]), T2-weighted imaging (9000/132), and fluid-attenuated inversion recovery (FLAIR) imaging (8000/110/2500 [TR/TE/TI]). MR images revealed that the brain morphology was normal, without any atrophic or edematous feature, in supratentorial areas and in the posterior fossa. Forceps-related extracerebral hemorrhage was present on the right temporal convexity, but this was not clinically important. An encysted cavum septi pellucidum was

Received March 21, 2001; accepted after revision September 26.

From the Centre de Résonance Magnétique en Biologie et Médecine-UMR-CNRS 6612 (A.V., S.C.-G., J.-P.R., P.J.C.), Faculté de Médecine, Service de Neuropédiatrie (B.C., F.V.), Hôpital la Timone, and Service de Neuroradiologie (C.R.), Hôpital la Timone, Marseille, France.

This work was supported by grants from the Centre National de la Recherche Scientifique (CNRS), the Association pour le Développement des Recherches Biologiques et Médicales au CHR de Marseille (ADEREM), and Institut Universitaire de France (IUF).

Address reprint requests to P. J. Cozzone, Centre de Résonance Magnétique en Biologie et Médecine-UMR-CNRS 6612, Faculté de Médecine la Timone, 27, bvd Jean Moulin, 13010 Marseille, France.

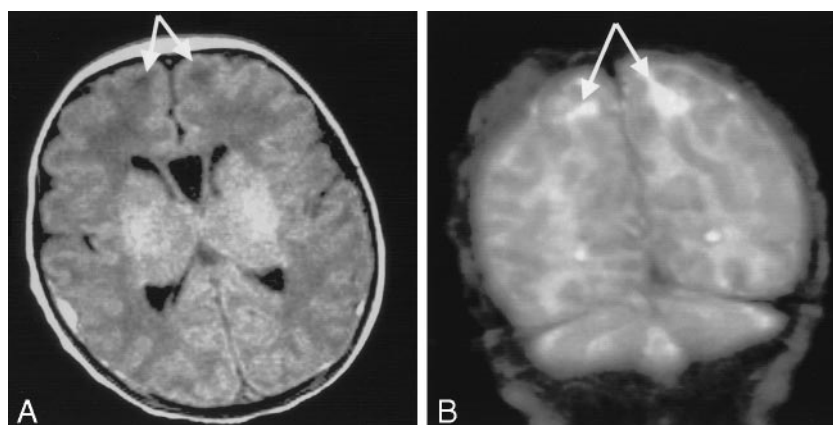


FIG 1. MR images.

A, Axial T1-weighted image of the basal ganglia shows small delivery-related hemorrhage over the temporal convexity and bilateral areas (arrows) of low signal intensity in the white matter of the most anterior portion of the superior frontal gyrus. Hypointense areas are more pronounced on the left. Note the encysted cavum septi pellucidi.

B, Coronal T2-weighted image shows bilateral areas (arrows) of high signal intensity in the superior parietal lobules. Hyperintense areas are more pronounced on the left.

present; it may have been benign, but this is also a common finding in metabolic brain diseases. The overall myelination of the brain was consistent with the gestational age of the neonate. The most important findings were areas of abnormally high signal intensity on T2-weighted images and abnormally low signal intensity on T1-weighted images of the subcortical white matter in the superior frontal gyrus and the superior parietal lobule in both hemispheres. These areas were symmetric but more pronounced on the left side than on the right (Fig 1). No signal intensity abnormality was found in the cerebellum.

Proton MR spectroscopy was performed by using the stimulated echo-acquisition mode (STEAM) sequence (1500/20; mixing time, 10 milliseconds) in a voxel of interest of  $2 \times 2 \times 2 \text{ cm}^3$  in the occipitoparietal white matter. Because of the small size of the regions with affected myelin on T2-weighted images, no spectra in the abnormal white matter could be recorded exclusively. Data processing consisted of zero-filling (2058 points), gaussian filtering (2 Hz), Fourier transformation, zero-order phase correction, and manual baseline correction. The spectra were referenced to creatine (3.04 ppm). The signals from *myo*-inositol (Ins) and glycine (Gly), choline (Cho), creatine and phosphocreatine (tCr), and *N*-acetylaspartate (NAA) were integrated. Results were expressed as ratios of the areas for the metabolites (NAA/tCr, Cho/tCr, Ins-Gly/tCr). Age-related curves for the cerebral metabolites, calculated from short-TE spectra published by Kreis et al (8), were used to provide normal values from age-matched control subjects. This comparison was possible because similar methods and conditions were used (STEAM sequence performed in the parietal white matter [1500/30; mixing time, 13 milliseconds]).

The signal amplitude of glutamine and glutamate (Glx) was substantially higher when a TE of 20 milliseconds was used; therefore, the Glx/tCr ratios were not compared. The integration values were not corrected for T1 or T2 effects (8). Two-dimensional (2D) spin-echo spectroscopic images were obtained with an acquisition-weighted 2D chemical-shift imaging (CSI) sequence (1500/135; matrix size,  $21 \times 21$ ; section thickness, 15 mm; FOV,  $240 \times 240 \text{ mm}$ ). Data processing consisted of zero-filling (2058 points), gaussian filtering (2 Hz), Fourier transformation, zero-order phase correction, manual baseline correction, and numeric integration. The metabolic pattern observed in the STEAM spectrum obtained in the normal-appearing white matter of the patient with RCDP at age 16 days (40 weeks' gestational age) showed that the dominant signal was from Ins-Gly, whereas the NAA level was low relative to that of the other metabolites (Fig 2). Taurine and *scyllo*-inositol were absent from the STEAM spectrum. When compared with spectra from the literature, the Glx signal amplitude seemed low (8–11).

Levels of mobile lipids were notably elevated. A signal assigned to acetate was also observed ( $\delta\text{ppm}$ , 1.95). Lactate was not detected on the STEAM spectrum or on spectra recorded with the CSI sequence (TE, 135 milliseconds) in either occipitoparietal white matter or gray matter (Fig 3). The value of Ins-Gly/tCr was significantly higher than in age-matched control subjects, whereas the Cho/tCr value was lower (Table). The CSI spectra obtained in both occipitoparietal white matter and gray matter essentially revealed the presence of a high Ins-Gly content (Fig 2, Table). In both spectra, the signal from aliasing lipids, presumably due to fat in the skull, was detected. The tCr value seemed lowered in CSI spectra in the gray matter, compared with the spectrum (TE, 135 milliseconds) that Grodd et al (11) recorded in the occipital gray matter of a 1-month-old healthy infant. However, because of the variability of tCr concentration in occipital gray matter of newborns (8), no definite conclusion can be drawn.

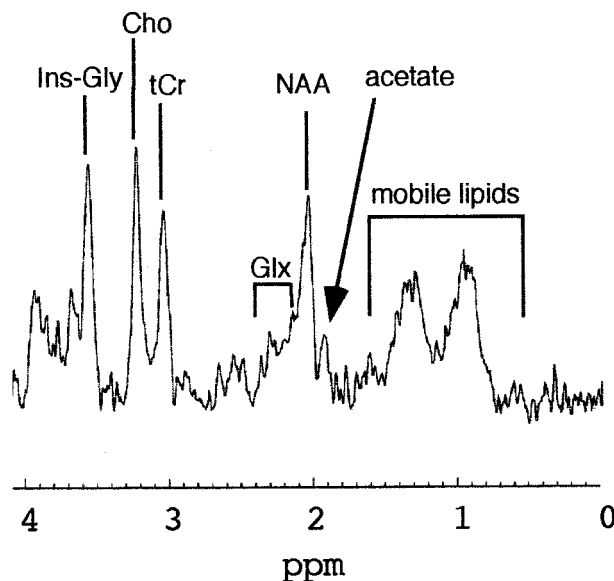
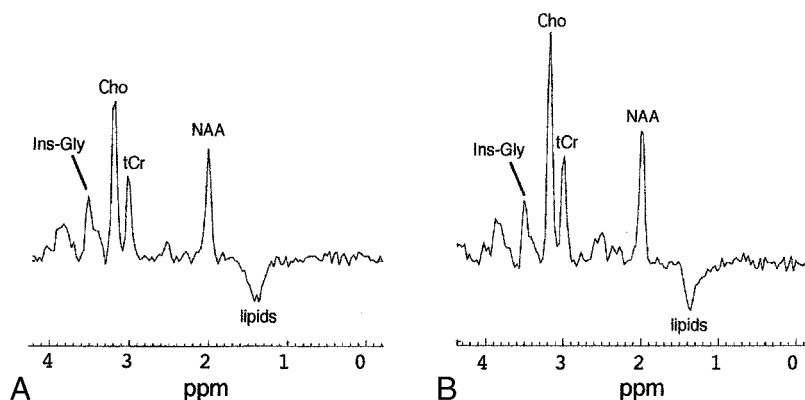


FIG 2.  $^1\text{H}$  MR spectrum obtained with the STEAM sequence (TE, 20 milliseconds) in the occipitoparietal white matter. The dominant feature of the spectrum is the high lipid and Ins-Gly content. The presence of an unusual resonance at 1.95 ppm was detected and assigned to acetate.

*in vitro*  $^1\text{H}$  MR spectroscopy of the blood serum was performed at 400 MHz, according to a method detailed in a previous article (12). An internal standard for chemical shift and concentration, namely 3-(trimethylsilyl)propionate-2,2,3,3-*d*4, was used. Reference values for blood serum were obtained with  $^1\text{H}$  MR spectroscopy in a group of 15 children (age range, 2–15 years) who had been admitted to the hospital with a suspected neurologic disorder; further examination findings confirmed the absence of neurologic disease. (A large-scale investigation of healthy neonates, infants, and children is still

FIG 3. Long-TE (135 milliseconds)  $^1\text{H}$  spectra obtained at 1.5 T with the CSI sequence in the occipitoparietal region. The main feature common to both spectra is the high Ins-Gly content.

A, Gray matter.  
B, White matter.



#### Brain metabolite analysis

White Matter Ratio	Value in the Patient with RCDP*	Control Value†
NAA/tCr	1.27	1.10
Cho/tCr	1.21	1.40
Ins-Gly/tCr	1.46	1.10

Note.—STEAM spectra with a TE of 20 milliseconds.

\* At 40 weeks' gestational age.

† From reference 14.

needed; this would be helpful to precisely define age-related metabolite concentrations in blood; however, such an investigation is not ethically acceptable.)  $^1\text{H}$  MR spectroscopy of the blood serum revealed a high concentration of lactate (3.52 mM; control value,  $2.12 \text{ mM} \pm 0.29$ ) (Fig 4). An elevated concentration of creatine (130  $\mu\text{M}$ ; control value,  $40 \mu\text{M} \pm 20$ ) was observed. The glutamine value was within the normal range. The glutamate level was visible, although it is usually not detectable on the proton spectrum of normal serum. Finally, all the ketone bodies, including acetone, acetate, acetoacetate, and  $\beta$ -hydroxybutyrate, were either in the normal range or not detectable (Fig 4).

#### Discussion

The reports (3, 13, 14) about peroxisomal disorders, such as Zellweger syndrome, X-linked adrenoleukodystrophy, and neonatal adrenoleukodystrophy, mention markedly elevated concentrations of Ins-Gly, Glx, and lactate in affected white matter, which reflect demyelination and glial proliferation. High concentrations of Ins-Gly in normal-appearing white matter have also been described. An increased level of mobile lipids in the white matter is a typical feature of Zellweger syndrome. No lactate was detected on brain spectra, although an increase in blood lactate levels was observed. Secondary hyperlactacidemia is a frequent feature in metabolic disorders, including peroxisomal diseases, but the cause remains unclear. In the current study, the STEAM spectrum recorded in the white matter was characterized by reduced levels Cho-containing compounds and high levels of Ins-Gly and mobile lipids. The high levels of Ins-Gly, as well as the presence of mobile lipids, are common features in the brains of healthy neonates. However, their levels appear substantially increased in the brain

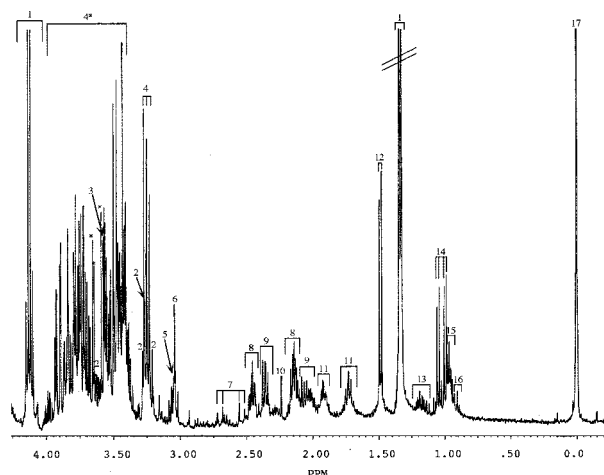
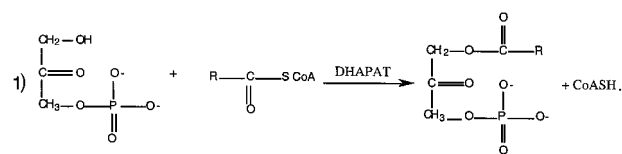


FIG 4.  $^1\text{H}$  MR spectrum in blood serum analyzed at 400 MHz shows a high concentration of lactate, creatine, and glutamate, whereas ketone body levels are normal. 1 indicates lactate; 2, *myo*-inositol; 3, glycine; 4, glucose; 4\*, mostly glucose; 5, creatinine; 6, creatine; 7, citrate; 8, glutamine; 9, glutamate; 10, acetone; 11, lysine; 12, alanine; 13, butyrate, valerate, malonate, and succinate derivatives; 14, valine; 15, leucine; 16,  $\alpha$ -hydroxybutyrate; 17, 3-(trimethylsilyl)propionate-2,2,3,3- $d_4$ ; \*, traces of glycerol from ultrafiltration.

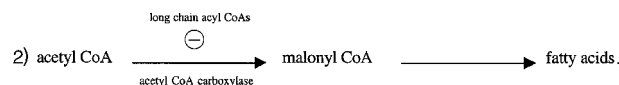
spectrum of this patient with RCDP, compared with that of neonates whose brain spectra have been published in the literature (8–10). Since *myo*-inositol is a glial marker, the increase in Ins-Gly might reflect some activation of glial cells, as observed in other peroxisomal diseases. The high content of brain lipids detected in the patient with RCDP presumably is a result of the deficient DHAPAT. DHAPAT, an enzyme present in all animal cells (except erythrocytes), catalyzes the esterification of dihydroxyacetone phosphate by long-chain acyl CoAs (more than 10 carbons) to form acyl DHAP, the precursor of plasmalogens (15), as follows (Eq 1):





Therefore, the increase in mobile lipids in the white matter of the patient with RCDP could directly reflect the accumulation of long chain acyl CoAs. Very-long-chain fatty acids (22, 24, or 26 carbon atoms) were normal in the patient with RCDP. However we cannot exclude, in view of the  $^1\text{H}$  MR spectroscopic findings, the possible accumulation of long chain fatty acids and their acyl derivatives, such as palmitate (16 carbon atoms) and stearate (18 carbon atoms), the preferred substrates for DHAPAT (15). Moreover, a previous study (16) has shown the accumulation of hexadecanol (the fatty alcohol derivative of palmitate) in plasma and cultured skin fibroblasts from six patients with RCDP, which was the result of their impaired incorporation into ether lipids. Another interesting finding is the elevated concentration of the acetate signal in the brain. To our knowledge, this is the first report of increased acetate levels in a neonatal brain proton spectrum, despite the many findings that a milk diet rich in fat provides ketone bodies that the developing brain takes up as primary fuel for respiration and as a carbon source for lipid synthesis (17). However, a  $^1\text{H}$  MR spectroscopic study (18) has revealed an increased acetate concentration in the cerebellum of suckling rats as a consequence of a milk diet. Ketone bodies are formed within the liver when fat degradation predominates, and they are supplied to the extrahepatic tissues via blood circulation. Therefore, high levels of blood ketone bodies are found with elevated brain acetate levels in suckling rats (18).

In this patient with RCDP,  $^1\text{H}$  MR spectroscopy of blood showed that ketone bodies, including acetone, acetoacetate, and acetate, were not detectable or within the normal range. This result suggests that the metabolite level at 1.95 ppm is not a consequence of the milk diet, but rather, it is produced within the brain. Previous studies (19) have shown that, in cultures, astrocytes can produce ketone bodies from fatty acids. Consequently, the fatty acids that accumulated in brain because of the DHAPAT deficiency could be degraded, and this lead to the formation of acetate. Moreover, astrocytes and oligodendrocytes are known to express acetyl CoA carboxylase (EC 6.4.1.2), the rate-limiting enzyme that regulates fatty acid synthesis and that is also involved in myelination. Long-chain acyl CoAs are potent inhibitors of acetyl CoA carboxylase (15). Thus, the accumulation of long-chain acyl CoAs could result in the inhibition of acetyl CoA carboxylase, thereby diverting acetyl CoA from fatty acid synthesis to acetate formation via hydrolysis by acetyl CoA hydrolase (EC 3.1.2.2), as follows (Eq 2):



No ketone bodies other than acetate have been detected in the brains of this patient with RCDP.

The importance of this increase in acetate levels, whether maturational or linked to DHAPAT deficiency, needs further investigation. Finally, the reduced concentration of Cho-containing compounds in the white matter is presumably a sign of hypomyelination resulting from the lack of plasmalogens for myelin synthesis.

## Acknowledgments

The authors thank Yann Le Fur for his help with the CSI sequence and Patrick Viout for technical assistance.

## References

1. Powers JM, Moser HW. **Peroxisomal disorders: genotype, phenotype, major neuropathologic lesions and pathogenesis.** *Brain Pathol* 1998;8:101–120
2. Wanders RJA. **Peroxisomal disorders: clinical, biochemical and molecular aspects.** *Neurochem Res* 1999;24:565–580
3. Bruhn H, Kruse B, Korenke GC, et al. **Proton NMR spectroscopy of cerebral metabolic alterations in infantile peroxisomal disorders.** *J Comput Assist Tomogr* 1992;16:335–344
4. Williams DW, Elster AD, Cox TD. **Cranial MR imaging in rhizomelic chondrodysplasia punctata.** *AJNR Am J Neuroradiol* 1991;12:363–365
5. Sztriha L, Al-Gazali LI, Wanders RJ, Ofman R, Nork M, Lestrinant GG. **Abnormal myelin formation in rhizomelic chondrodysplasia punctata type 2 (DHAPAT-deficiency).** *Dev Med Child Neurol* 2000;42:492–495
6. van der Knapp MS, Valk J. **The MR spectrum of peroxisomal disorder.** *Neuroradiology* 1991;33:30–37
7. Lenti C, Paganoni P, Sangermani R. **Rhizomelic chondrodysplasia punctata: 16-year follow-up of a child from birth.** *Ital J Neurol Sci* 1991;12:469–473
8. Kreis R, Ernst T, Ross BD. **Development of the human brain: in vivo quantification of metabolite and water content with proton magnetic resonance spectroscopy.** *Magn Res Med* 1993;30:424–437
9. Ross BD, Kreis R, Ernst T. **Clinical for the 90s: magnetic resonance spectroscopy and metabolite imaging.** *Eur J Radiol* 1992;14:128–140
10. Hüppi PS, Barnes PD. **Magnetic resonance techniques in the evaluation of the newborn brain.** *Clin Perinatol* 1997;24:693–723
11. Grodd W, Krageloh-Mann I, Klose U, Sauter R. **Metabolic and destructive brain disorders in children: findings with localized proton MR spectroscopy.** *Radiology* 1991;181:173–181
12. Maillet S, Vion-Dury J, Confort-Gouny S, et al. **Experimental protocol for clinical analysis of cerebrospinal fluid by high resolution proton magnetic resonance spectroscopy.** *Brain Res Brain Res Protoc* 1998;3:123–134
13. Pouwels PJ, Kruse B, Korenke GC, Mao X, Hanefeld FA, Frahm J. **Quantitative proton magnetic resonance spectroscopy of childhood adrenoleukodystrophy.** *Neuropediatrics* 1998;29:254–264
14. Confort-Gouny S, Vion-Dury J, Chabrol B, Nicoli F, Cozzzone PJ. **Localized proton magnetic resonance spectroscopy in X-linked adrenoleukodystrophy.** *Neuroradiology* 1995;37:568–575
15. Hajra AK. **Dihydroxyacetone phosphate acyltransferase.** *Biochim Biophys Acta* 1997;1348:27–34
16. Rizzo WB, Craft DA, Judd LL, Moser HW, Moser AB. **Fatty alcohol accumulation in the autosomal recessive form of rhizomelic chondrodysplasia punctata.** *Biochem Med Metab Biol* 1993;50:93–102
17. Edmond J. **Energy metabolism in developing brain cells.** *Can J Physiol Pharmacol* 1992;70(suppl):S118–S129
18. Martin M, Merle M, Labouesse J, Canioni P. **Postnatal decrease of acetate concentration in rat cerebellum.** *J Neurosci Res* 1994;37:103–107
19. Auestad N, Korsak RA, Morrow JW, Edmond J. **Fatty acid oxidation and ketogenesis by astrocytes in primary culture.** *J Neurochem* 1991;56:1376–1386